Available online at www.sciencedirect.com
SCIENCE DIRECT®

Journal of the European Ceramic Society 23 (2003) 1175–1182
www.elsevier.com/locate/jeurceramsoc

Effect of large β-Si_3N_4 particles on the thermal conductivity of β-Si_3N_4 ceramics

H. Yokota*, S. Yamada, M. Ibukiyama

Research Center, Denki Kagaku Kogyo K.K, 3-5-1 Asahi-cho, Machida-city, 194-8560 Tokyo, Japan

Received 16 November 2001; received in revised form 22 July 2002; accepted 7 August 2002

Abstract

Mean-field micromechanics model, the rule of mixture is applied to the prediction of the thermal conductivity of sintered β-Si_3N_4, considering that the microstructure of β-Si_3N_4 is composed of a uniform matrix phase (which contains grain boundaries and small grains of Si_3N_4) and the purified large grains ($\geqslant 2$ μm in diameter) of Si_3N_4. Experimental results and theoretical calculations showed that the thermal conductivity of Si_3N_4 is controlled by the amount of the purified large grains of Si_3N_4. The present study demonstrates that the high thermal conductivity of β-Si_3N_4 can be explained by the precipitation of high purity grains of β-Si_3N_4 from liquid phase.

Keywords: Grain growth; Grain size; Sintering; Si_3N_4; Thermal conductivity

1. Introduction

Recently, a significant increase in the thermal conductivity, the value has been exceeded 100 W $(m\ K)^{-1}$, of sintered β-Si_3N_4 has been achieved by using high-purity raw powders with effective sintering additives.[1–6] These results suggest that the thermal conductivity of sintered Si_3N_4 is closely related to both purity of Si_3N_4 grains and the microstructure of the sintered material.

The conduction of heat in ceramics is dominated by phonon transport. Watari et al.[7] reported that the thermal conductivity of Si_3N_4 at room temperature is independent of grain size, but controlled by the internal defect structure of the grains such as point defects and dislocations. It is known that the phonon scattering is attributed to imperfections in the crystal lattice such as impurities, vacancies, interstitials and dislocations at room temperatures.[8] Kitayama et al.[9] concluded that the point defects in the β-Si_3N_4 crystal lattice that are created by oxygen dissolution dictate the thermal conductivity of that material. Kitayama et al.[9] also concluded that the grain boundary phase compositions, originated from liquid phase composition during the grain growth, dictate the lattice oxygen content of β-Si_3N_4. In a previous work,[10,11] it was reported that a precise chemical analysis of sintered β-Si_3N_4 grains was performed, as a result, the major impurity in the grains was oxygen, but the content of oxygen as well as of metal impurities except lattice aluminum in the β-Si_3N_4 grains decreased with the grain growth. It is because the impurities in the grains were partially eliminated by the dissolution-reprecipitation via liquid phase with grain growth. Thus, the purity of the Si_3N_4 grains is closely related to grain growth with the appropriate sintering additives.

Theoretical models for the prediction of the thermal conductivity of β-Si_3N_4 have been attempt. Hirao et al.[3] demonstrated that the relationship between the area fraction of elongated grains and thermal conductivity accurately follows Wiener parallel and serial formulas[12] for the thermal conductivity of a composite material. Although Wiener model might be applicable to β-Si_3N_4 with a bimodal microstructure consisting of a fine matrix and large elongated grains, they are not sufficient to describe the thermal conductivity of β-Si_3N_4 without such a unique microstructure.[13] The formulas contain only the volume fractions of constituents and cannot treat the grain sizes and shape, arrangement of anisotropic grains that all characterized β-Si_3N_4. Kitayama et

* Corresponding author. Fax: +81-427-21-3693.
E-mail address: hiroshi-yokota@denka.co.jp (H. Yokota).

0955-2219/03/$ - see front matter
PII: S0955-2219(02)00291-1

al.[13] further investigated the effects of various microstructural factors (grain size, thickness of the grain boundary film, and alignment of elongated grains) of hot-pressed β-Si_3N_4 ceramics on thermal conductivity by using modified Wiener model. The model assumed that the thermal conductivity of β-Si_3N_4 crystal in the composite is always constant value. If the point defects in the β-Si_3N_4 crystal lattice that are created by oxygen dissolution dictate the thermal conductivity of β-Si_3N_4 ceramics, the thermal conductivity should depend on the grain size with purification. Therefore, the calculated value,[13] for the thermal conductivity in the region of small grain size is considered an overestimate, while the thermal conductivity is underestimated in the region of large grain size. Thus, the constant estimation value for the thermal conductivity of β-Si_3N_4 grains does not accurately represent the effective value for the thermal conductivity. Therefore, it is necessary to use an estimation value for the thermal conductivity taking into account the purity of the β-Si_3N_4 grains in the rule of mixture. The estimate for the thermal conductivity of each grain size of β-Si_3N_4 is difficult at this time.

In general, the sintered β-Si_3N_4 materials reveal the microstructure of self-reinforced composites consisting of some large elongated grains in fine matrix grains. The sintered materials are considered to be composed of the purified large grains, the impure small grains and the grain boundary phase,[10,11] so that it is highly possible that the amount and dispersed conditions of the large grains in the matrix phase have influence on the thermal conductivity of β-Si_3N_4 ceramics.

In the present work, the thermal conductivities of β-Si_3N_4 with different volume of the large grains were investigated. The results were compared with predictive models by modeling the thermal conductivity of β-Si_3N_4, roughly taking into account the purity of β-Si_3N_4 grain in the sintered materials.

2. Experimental procedure

All of the specimens were prepared from high-purity Si_3N_4 raw powders and sintering aids. The specifications of raw β-Si_3N_4 powders (Grade NP-400, Denki Kagaku Kogyo, Tokyo, Japan), obtained by direct nitridation of silicon are shown in Table 1. The individual raw silicon nitride powder and 8 mass% Y_2O_3 (purity > 99.9%, BET 4 m^2/g, Shin-etsu Chemical, Tokyo, Japan) and 1 mass% HfO_2 (purity > 99.9%, BET 4 m^2/g, Soekawa Chemical, Tokyo, Japan) were ball milled using methanol as the solvent for 3 h. After they were dried, the powder mixtures were prepared for sintering.

Approximately 2 g of the dried powder was uniaxially pressed under 20 MPa in a die 12.5 mm in diameter. The pellet was then isostatically cold-pressed under a pressure of 200 MPa. The CIPped pellet was placed in a BN crucible. Sintering was performed in a graphite furnace at 1900 °C for 4, 8, 20 and 48 h, respectively, under a nitrogen pressure of 0.9 MPa. The specimens sintered at 8 and 48 h were the same specimens which were described in the previous work.[10,11] The densities of specimens were measured by the Archimedes method. The microstructure of the sintered materials was examined by scanning electron microscopy (SEM, JSM-820, Jeol, Tokyo, Japan) of polished and CF_4 plasma etched surfaces

Table 1
Properties of raw Si_3N_4 powder

Property	NP-400
Purity	
Oxygen (mass%)	0.92
Aluminum (ppm)	80
Calcium (ppm)	230
Iron (ppm)	710
BET specific surface area (m^2 g^{-1})	19.0

To evaluate the thermal conductivity, the disks 10 mm in diameter and 3 mm in thickness were cut from sintered materials. Thermal conductivity at room temperature was calculated from the equation:

$$K = \alpha \; C_p \; \rho$$

The thermal diffusivity (α) and the specific heat (C_p) of the specimens were measured at room temperature, by the laser-flash method, using a thermal-constant analyzer (Model TC-3000, ULVAC Japan, Ltd., Tokyo, Japan). The specific heat (C_p) was about the same, independent of the sintering time. Therefore, the average value of 0.67 J (g K)$^{-1}$ was used in this work. Phase identification of the sintered materials was performed by X-ray diffractometry (XRD).

3. Results and discussion

3.1. Microstructural characterization

Two distinct SEM images were employed for one specimen. Fig. 1 shows SEM photographs of the polished and plasma-etched surfaces of the sintered specimens, which were observed at low magnification of 350× to evaluate relatively large grains ($\geqslant 2$ μm).

Fig. 2 also shows SEM photographs of the sintered specimens, which were observed at high magnification of 3500× to evaluate smaller matrix grains (< 2 μm). All specimens had a bimodal microstructure consisting of a lot of fine matrix grains and a number of large elongated grains. Area fraction of the large grains increased with sintering time.

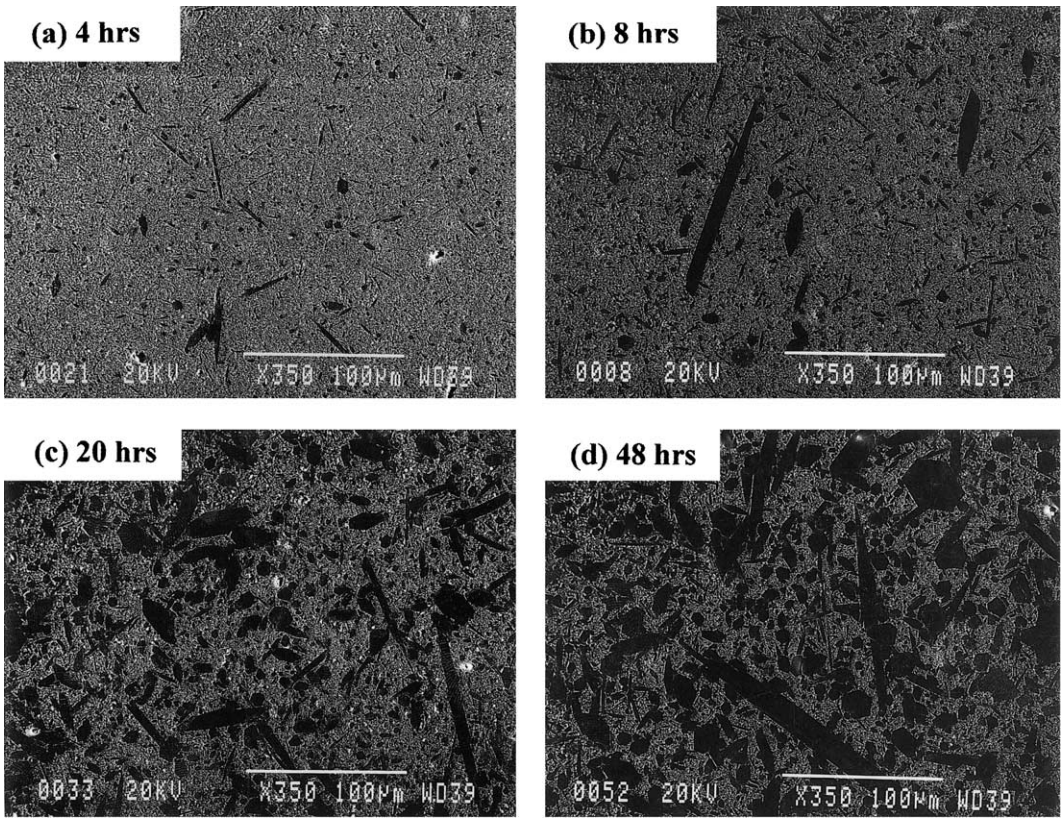

Fig. 1. Low magnification SEM photographs of polished and plasma-etched surface of the specimens sintered at 1900 °C for (a) 4 h specimen, (b) 8 h specimen, (c) 20 h specimen, (d) 48 h specimen.

Digital processing and analysis were performed to quantitatively characterize the microstructure with the wide-ranged grain size distribution. The two SEM images with the different magnification for one specimen were analyzed by image processor to measure length (longest dimension), diameter (shortest dimensions), and area fraction of each grain, and then synthesized into one distribution.[14]

Fig. 3 shows the grain size distribution of the sintered materials. The bimodal microstructure was also confirmed by the grain size distribution. Two peaks with the grain size of <2 μm and $\geqslant 2$ μm were clearly observed. The lower peak corresponds to the matrix grains and the upper peak corresponds to large elongated grains in the bimodal microstructure. Thus, the critical diameter for the definition of matrix grains and large grains is 2 μm. Purification nature by the solution-reprecipitation as grain growth of Si_3N_4 with 8 mass % of Y_2O_3 and 1 mass % of HfO_2, in particular remarkably purified in the region of <1 μm in diameter except in the case of the lattice aluminum, so that the large grains ($\geqslant 2$ μm in diameter) of the sintered materials are considered to be the purified. It was found that an area fraction of the large grains increased with sintering time, but the sintered for 48 hrs specimen still contained the impure matrix grains.[10,11] From these results, different amounts of the large grains were successfully obtained.

Table 2
Density, area fraction of large grains, mean size of large grains, aspect ratio of large grains, and thermal conductivities of β-Si_3N_4

Sintering conditions	Density (g/cm^3)	Area fraction of large grains (area%)	Mean size of large grains (μm)	Aspect ratio of large grains	Thermal conductivity [W (m K)$^{-1}$]
1900 °C, 4 h	3.31	3.5	0.5	4.8	87
1900 °C, 8 h	3.33	6.0	1.0	4.7	88
1900 °C, 20 h	3.32	32.2	5.4	3.6	109
1900 °C, 48 h	3.29	46.1	5.9	4.1	120

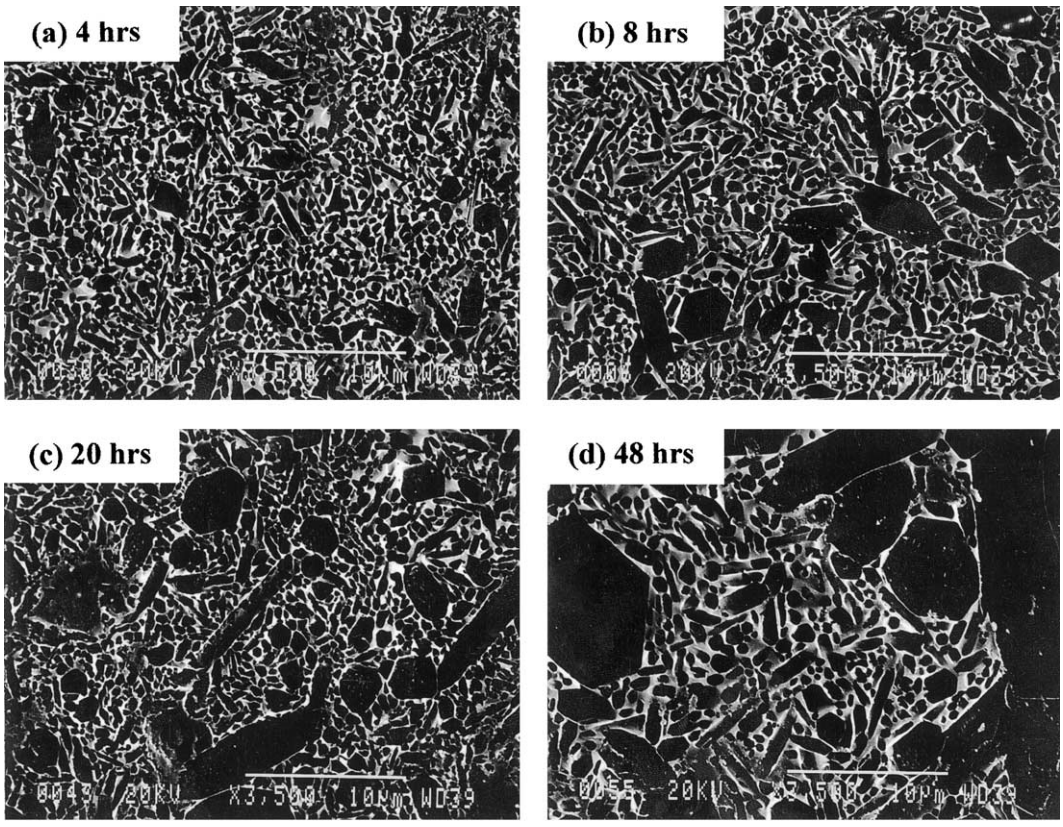

Fig. 2. High magnification SEM photographs of polished and plasma-etched surface of the specimens sintered at 1900 °C for (a) 4 h specimen, (b) 8 h specimen, (c) 20 h specimen, (d) 48 h specimen.

Table 2 shows density, area fraction of large grains, mean size of large grains, aspect ratio of large grains, and thermal conductivities of β-Si_3N_4. Table 2 reveals that the thermal conductivity of the specimens increased as the sintering time, the area fraction of large grains and the mean size of the large grains increased. The maximum thermal conductivity of the sintered material was obtained for the value of 120 W (m K)$^{-1}$.

Table 3 summarizes the results of the XRD phase identification for the specimens sintered from the both powders. For the specimen sintered from the 4, 8, 20 and 48 h, the $YSiO_2N$ phase as well as the $Y_2Si_3N_4O_3$ phase was observed, and the corresponding Y_2O_3/SiO_2 additive ratio was 2/1 and 1/0, respectively. It is therefore expected that the lattice oxygen removal can occur during grain growth.

3.2. Comparison to theoretical predictive models

Fig. 4(a) shows illustrations of typical 3D randomly oriented microstructure of sintered β-Si_3N_4, which is composed of large elongated grains, small grains, and grain boundary phase. Fig. 4(b) shows illustrations of idealized binary phase composite of sintered β-Si_3N_4, when assuming that the small grains and grain boundary phase are a uniform matrix phase regarded as the continuous phase. In this case the purified large grains are considered to be a dispersed phase. In this study, taking into account the purity of the β-Si_3N_4 grains, we distinguish the large grains ($\geqslant 2$ μm in diameter). It is impossible to perform a calculation based on a Maxwell model derived by Eucken[15] in terms of thermal conductivity of the composite material with randomly

Table 3
Results of grain boundary phase identification via XRD for specimens sintered at 4, 8, 20, and 48 h

Sintering conditions	Y_2SiO_5 $Y_2O_3/SiO_2 = 1/1$	$Y_{20}N_4Si_{12}O_{48}$ $Y_2O_3/SiO_2 = 10/9$	$YSiO_2N$ $Y_2O_3/SiO_2 = 2/1$	$Y_2Si_3N_4O_3$ $Y_2O_3/SiO_2 = 1/Ø$	$Y_2Hf_2O_7$
1900 °C, 4 h	((x))	(x)	xx	x	xx
1900 °C, 8 h	((x))	(x)	xx	x	xx
1900 °C, 20 h	((x))	(x)	x	x	xx
1900 °C, 48 h	((x))	(x)	x	xx	xx

xx = major content; x = small amount; (x), ((x)) = traces.

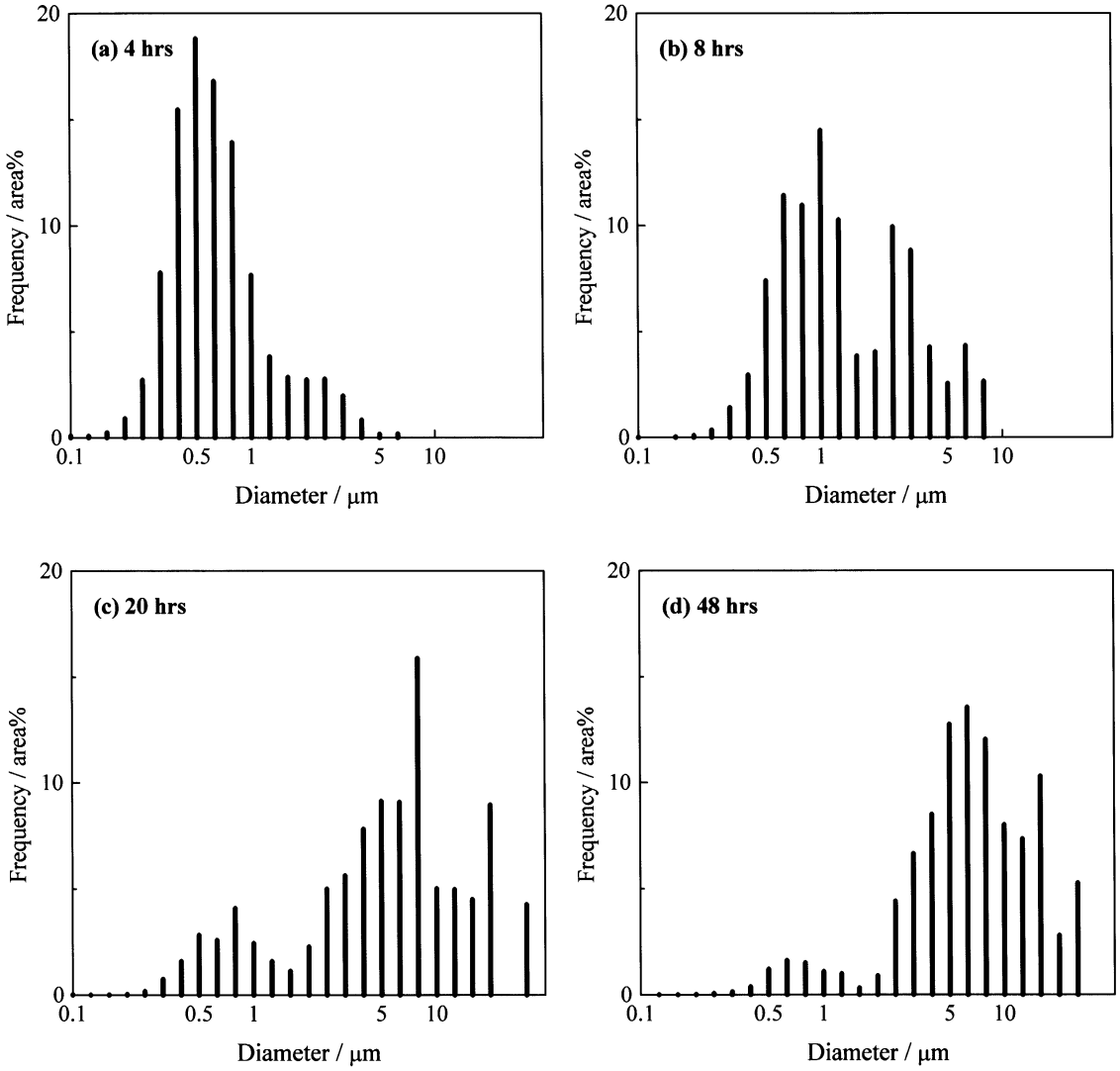

Fig. 3. Grain size distribution of the sintered materials of the specimens sintered at 1900 °C for (a) 4 h specimen, (b) 8 h specimen, (c) 20 h specimen, (d) 48 h specimen.

oriented microstructure, because the shape of the β-Si_3N_4 large grains is not regarded as sphere particles in the microstructure.

Wakashima and Tsukamoto[16] proposed a mean-field micromechanics model. The model is applied to the prediction of overall thermoelastic properties of some specific composite of practical interest. In the model, they showed a specific microstructural model, in which each of the discrete phases is represented by a group of numerous ellipsoidal particles of the same shape with corresponding axes aligned, as shown in Fig. 5. For the system with randomly oriented spheroidal particles in particular, the overall bulk and shear moduli, computed as a function of the particle aspect ratio, are shown to vary systematically within the margins which coincide with the bounds given by Hashin and Shtrikman.[17] They further extend their proposed models[16] to predict the effective thermal conductivities of composite materials with the binary phases containing perfectly aligned or randomly oriented microstructures.[18] Now, we can do calculations for the prediction of the thermal conductivity by using the following assumptions. Firstly, although thermal conductivity anisotropy might exist, we assume in this work that the thermal conductivity is independent of the crystallography. Secondly, we assume that the thermal resistance of the boundary between the large grains and the matrix phase is regarded to be negligible. Using the model for the thermal conductivity with randomly oriented microstructure, the thermal conductivity of the sintered materials, K is expressed by the following three equations:[18]

$$K = K_M + \frac{V_L\{A^0\}(K_L - K_M)}{(1 - V_L) + V_L\{A^0\}} \quad (1a)$$

$$3\{A^0\} = \sum_{k=1}^{3} \frac{K_M}{K_M + S^{(K)}(K_L - K_M)} \quad (1b)$$

$$S^{(3)} = 1 - 2S^{(1)}, S^{(1)} = S^{(2)} = \frac{(x/2)\left[x\sqrt{x^2-1} - \cosh^{-1}x\right]}{\left(\sqrt{x^2-1}\right)^3} \quad (1c)$$

where K_M, K_L, V_L, $\{A^0\}$, S^K and χ are the thermal conductivity of the matrix phase, the thermal conductivity of the large grains, the volume fraction of the large grains, average value of concentration factor,[18] shape factor (Eshelby's tensor),[19,20] and aspect ratio of the large grains, respectively. The shape factor is a function of the geometry (aspect ratio) of the large grains. The area fraction for planar surfaces statistically corresponds to volume fraction,[14] so that we substitute the area fraction of the large grains for the V_L. Since we assume the sintered materials as the two-phase composite material, the volume fraction of the matrix phase is presented as $(1-V_L)$. Combining Eqs. (1a)–(1c) makes it possible to describe the thermal conductivity of sintered β-Si_3N_4. The components of Wakashima's prediction model[18] (also the definitions of the concentration factor, shape factor) are given in the Appendix.

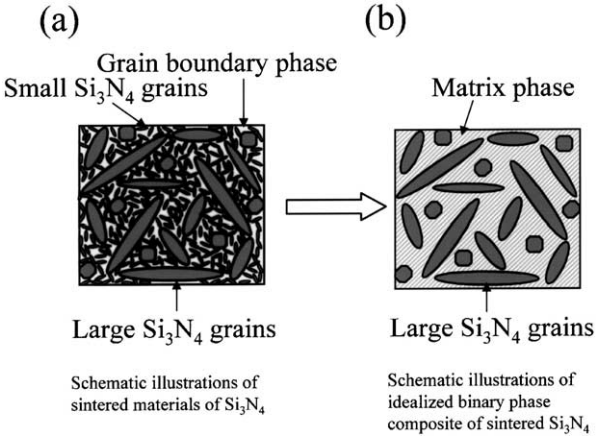

Fig. 4. (a) Illustrations of typical 3D randomly oriented microstructure of sintered β-Si_3N_4, which composed, of the large elongated grains, small grains, and grain boundary phase. (b) Illustrations of idealized binary phase composite of sintered β-Si_3N_4, when assuming that the small grains and grain boundary phase are a uniform matrix phase regarded as the continuous phase.

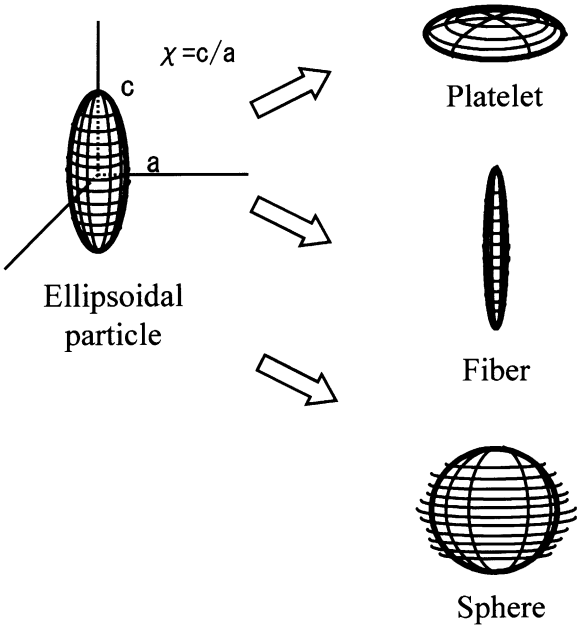

Fig. 5. Schematic illustration of the microgeometrical features of the mean-field micromechanics model.

Fig. 6 compares the calculated and experimental results, when the grain aspect ratio χ is chosen for 4.3 (the mean value of the four specimens in Table 2). When $\chi = 4.3$ is chosen, the calculated value by the Eqs. (1b) and (1c) of the $S^{(1)}$, $S^{(2)}$, $S^{(3)}$, and $\{A^0\}$ are 0.4657, 0.4657, 0.0685, 0.7573, respectively. Fig. 6 shows that the thermal conductivities of the β-Si_3N_4 increase as the amount of large grain increase (indicated by the circular plots "exp. data" in Fig. 6). Assuming the (K_L/K_M) of (175/85) results in a good fit to the experimental data (indicated by the straight line "model" in Fig. 6), supporting the argument that the β-Si_3N_4 can be regarded as a two phase composite in which large grains with high thermal conductivity are dispersed within the matrix phase of low thermal conductivity. This result suggests that the reprecipitated large grains ($\geqslant 2$ μm) have a higher thermal conductivity because of its purity. It is likely that the large β-Si_3N_4 grains can undergo

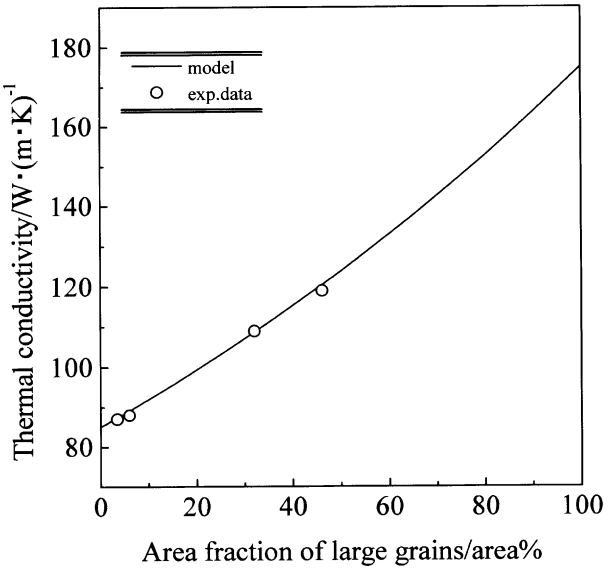

Fig. 6. Comparing the calculated and experimental results—the thermal conductivities of the sintered β-Si_3N_4 as a function of the amount of the large grains.

purification via the liquid phase during the sintering, so that the large grains have less impurity content than the small grains. [11] In the liquid phase sintering, smaller grains, originally impure (containing a higher concentration of impurities[11]), can dissolve in the liquid and deposit as purer β-Si_3N_4 (containing equilibrium concentration of oxygen and lattice aluminum[11]) on larger grains. Hence, these results support the conclusion that enhancement in thermal conductivity with sintering time is attributed to the precipitation of the purified large β-Si_3N_4 grains.

The theoretical calculation and experimental results suggest that the thermal conductivity for the β-Si_3N_4 does not exhibit a well-defined percolation threshold (the volume fraction which rapidly increases the thermal conductivity). This is because that there does not remarkably exist the large difference in component thermal conductivity values, such as found in the filler composite composed of 0.2 W (m K)$^{-1}$ of polyimide matrix and 28 W (m K)$^{-1}$ of alumina.

4. Conclusions

The sintered materials were prepared by the use of the high-purity β-Si_3N_4 powder sintered at 1900 °C for 4, 8, 20 and 48 h with the addition of 8 mass % Y_2O_3 and 1 mass % HfO_2. The following conclusions can be determined, based on the present work.

1. The grain size distributions of the sintered materials exhibited bimodal microstructures. Two peaks with the grain size of <2 μm and $\geqslant 2$ μm were clearly observed. The lower peak corresponds to the matrix grains with less pure than the large grains and the upper peak corresponds to large elongated with purified grains.
2. The thermal conductivity increased with purity of the large grains ($\geqslant 2$ μm in diameter) of β-Si_3N_4.
3. The mean-field micromechanics model gives reasonable prediction of the thermal conductivity with roughly taking into account the purity of β-Si_3N_4 grain in the sintered materials.
4. The sintered materials can be regarded as a two phase composite in which large grains with high thermal conductivity are dispersed within the matrix phase of low thermal conductivity.
5. The theoretical calculation and experimental results suggest that the thermal conductivity for the β-Si_3N_4 does not exhibit a well-defined percolation threshold.

Overall, the present work has demonstrated that the high thermal conductivity of β-Si_3N_4 can be explained by the precipitation of purity grains of β-Si_3N_4 from liquid phase.

Appendix

Wakashima et al. was used to estimate the effective thermal conductivity of a multi phase system characterized by a random dispersion of N different sets of arbitrary oriented spheroidal particles in an isotropic matrix. When the phase 0 is a continuous matrix phase, in which all other phases ($r=1,2,\ldots N$) are embedded as randomly oriented spheroidal particles which have different aspect ratios $\chi = c/a$, the effective thermal conductivity K of the composite material is presented as

$$K = \sum_{r=0}^{N} f_r K_r A_r \tag{A1}$$

where K: the effective thermal conductivity of the composite; f_r: volume fraction of the spheroidal particles; K_r: the thermal conductivity of the spheroidal particles; A_r: the concentration factor (A_r must satisfy $\sum_{r=0}^{N} f_r A_r = I$); I: unit tensor.

Here A_r is a second-rank tensor, called the concentration factor. A_r is defined as

$$\langle H \rangle_r = A_r \langle H \rangle \tag{A2}$$

where $<H>$ is a mean temperature gradient in the macroscopic range, $<H>_r$ is a mean temperature gradient in the individual phases.

For a two phase system, i.e. $r=0$ and $r=1$, in particular, Eq. (A1) is represented as

$$(K_1 - K_0)^{-1}(K - K_0) = f_1 A_1 \tag{A3}$$

where K_0: the thermal conductivity of the matrix phase.

Here the concentration factor is presented which is taken into account with the "mean-field approximation" by

$$A_r = A_r^0 \left(\sum_{r=0}^{N} f_r A_r^0 \right)^{-1} \tag{A4}$$

Also the A_r^0 is represented as

$$A_r^0 = \left[I + S_r K_0^{-1} (K_r - K_0) \right]^{-1} \tag{A5}$$

where S_r: shape factor of the spheroidal particles (Eshelby's tensor).

Eq. (A3) is represented by using Eq. (A4):

$$(K_1 - K_0)^{-1}(K - K_0) = f_1 A_1^0 \left(f_0 A_0^0 + f_1 A_1^0 \right)^{-1} \tag{A6}$$

Eq. (A6) is represented by using Eq. (A5) as

$$\begin{aligned}(K_1-K_0)^{-1}(K-K_0) &= f_1A_1^0\left(f_1I+f_1A_1^0\right)^{-1}\\ &= f_1\left[\left(f_0I+f_1A_1^0\right)\left(A_1^0\right)^{-1}\right]^{-1}\\ &= f_1\left[f_0\left(A_1^0\right)^{-1}+f_1I\right]^{-1}\\ &= f_1\left[I+f_0SK_0^{-1}(K_1-K_0)\right]^{-1}\end{aligned} \quad \text{(A7)}$$

Here, the shape factor S_r (Eshelby's tensor), as a function of the aspect ratio χ of the spheroid, is given as

$$\begin{aligned}S_{11} = S_{12} &= \frac{1-S_{33}}{2}\\ &= \frac{\frac{\chi}{2}\left[\chi\sqrt{\chi^2-1}-\cosh^{-1}\chi\right]}{\left(\sqrt{\chi^2-1}\right)^3}\end{aligned} \quad \text{(A8)}$$

For two-phase material made up of randomly oriented spheroidal particles which have isotropic thermal conductivities, the effective thermal conductivity of the composite is obviously isotropic (thus, $K^{(1)}=K^{(2)}=K^{(3)}$).

In this case, Eq. (A6) is represented by using of $\{A_r^0\}$ as,

$$(K_1-K_0)^{-1}(K-K_0) = f_1\left\{A_r^0\right\}\left(f_0I+f_1\left\{A_r^0\right\}\right)^{-1} \quad \text{(A9)}$$

where $\{A_r^0\}$ is an orientational average of overall directions of the A_r^0. Then Eq. (A9) yields as:

$$\begin{aligned}\frac{K^{(K)}-K_0}{K_1-K_0} &= \frac{f_1\left\{A_1^0\right\}}{f_0+f_1\left\{A_1^0\right\}}\\ K^{(K)} &= K_0+\frac{f_1\left\{A_1^0\right\}}{f_0+f_1\left\{A_1^0\right\}}(K_1-K_0)\end{aligned} \quad \text{(A10)}$$

Here the A_1^0 is given as

$$3\left\{A_1^0\right\} = \sum_{k=1}^{3}\frac{K_0}{K_0+S^{(K)}(K_1-K_0)} \quad \text{(A11)}$$

Thus the thermal conductivity of the two-phase composite material with randomly oriented spheroidal particles can be calculated by Eqs. (A10), (A11) and (A8).

References

1. Hirosaki, N., Okamoto, Y., Ando, M., Munakata, F. and Akiume, Y., Thermal conductivity of gas-pressure-sintered silicon nitride. *J. Am. Ceram. Soc.*, 1996, **79**(11), 2878–2882.
2. Hirosaki, N., Okamoto, Y., Ando, M., Munakata, F. and Akiume, Y., Effect of grain growth on the thermal conductivity of silicon nitride. *J. Ceram. Soc. Jpn*, 1996, **104**(1), 49–53.
3. Hirao, K., Watari, K., Brito, M. E., Toriyama, M. and Kanzaki, S., High thermal conductivity in silicon nitride with anisotropic microstructure. *J. Am. Ceram. Soc.*, 1996, **79**(9), 2485–2488.
4. Watari, K., Hirao, K., Brito, M. E., Toriyama, M. and Kanzaki, S., Hot isostatic pressing to increase thermal conductivity of silicon nitride ceramics. *J. Mater. Res.*, 1999, **14**(4), 1538–1541.
5. Akiume, Y., Munakata, F., Matsuo, K., Okamoto, Y., Hirosaki, N. and Satoh, C., Effect of grain size and grains structure on the thermal conductivity of β-Si_3N_4. *J. Ceram. Soc. Jpn*, 2000, **83**(8), 1985–1992.
6. Hayashi, H., Hirao, K., Toriyama, M., Kanzaki, S. and Itatani, K., $MgSiN_2$ addition as a means of increasing the thermal conductivity of β-Silicon nitride. *J. Am. Ceram. Soc.*, 2001, **84**(12), 3060–3062.
7. Watari, K., Hirao, K., Brito, M. E., Toriyama, M. and Ishizaki, K., Effect of grain size on the thermal conductivity of silicon nitride. *J. Am. Ceram. Soc.*, 1999, **82**(3), 777–779.
8. Kingery, W. D., The thermal conductivity of ceramic dielectrics. In *Progress in Ceramic Science, Vol.2*, ed. J. E. Burke. Pergamon Press, New York, 1962, pp. 182–235.
9. Kitayama, M., Hirao, K., Tsuge, A., Watari, K., Toriyama, M. and Kanzaki, S., Thermal conductivity of β-Si_3N_4. Part II, effect of lattice oxygen. *J. Am. Ceram. Soc.*, 2000, **83**(8), 1985–1992.
10. Yokota, H. and Ibukiyama, M., High-thermal conductivity of β-Si_3N_4 prepared by gas pressure sintering. In *Ceramic Transactions, Vol 112, Ceramic Processing Science IV, 7th International Ceramic Processing Science Meeting 2000*, ed. S. Hirano, G. L. Messing and N. Claussen. American Ceramic Society, Westerville, OH, 2001, pp. 611–616.
11. Yokota, H. and Ibukiyama, M. Effect of lattice impurities on the thermal conductivity of β-Si_3N_4. *J. Eur. Ceram. Soc.*, 2003, **23**(1), 55–60.
12. Wiener, O., Lamellare doppelbrechung. *Phys.Z*, 1904, **5**, 332–338.
13. Kitayama, M., Hirao, K., Toriyama, M. and Kanzaki, S., Thermal conductivity of β-Si_3N_4. Part I, effects of various microstructural factors. *J. Am. Ceram. Soc.*, 1999, **82**(11), 3105–3112.
14. Hirosaki, N., Akiume, Y. and Mitomo, M., Quantitative analysis of microstructure of self-reinforced silicon nitride ceramics. *J. Ceram. Soc. Jpn*, 1993, **101**(11), 1239–1243.
15. Francl, J. and Kingery, W. D., Thermal conductivity: IX, experimental investigation of effect of porosity on thermal conductivity. *J. Am. Ceram. Soc.*, 1954, **37**(2), 99–106.
16. Wakashima, K. and Tsukamoto, H., Mean-field micromechanics model and its application to the analysis of thermomechanical behavior of composite materials. *Mater. Sci. Eng.*, 1991, **A146**, 291–316.
17. Hashin, Z. and Shtrikman, S., A variational approach to the theory of the elastic behavior of multiphase materials. *J. Mech. Phys. Solids*, 1963, **11**, 127–140.
18. Wakashima, K., A theoretical approach to the prediction of effective thermal conductivities of composite materials. *Netsu. Bussei*, 1992, **6**(4), 255–264 (in Japanese).
19. Eshelby, J. D., *Proc. R. Soc. London*, 1957, **A241**, 376.
20. Eshelby, J. D., *Proc. R. Soc. London*, 1959, **A252**, 561.